ORIGINAL ARTICLE

Thiamine Deficiency Increases Intrinsic Excitability of Mouse Cerebellar Purkinje Cells

Ivonne Carolina Bolaños-Burgos[1] · Ana María Bernal-Correa[2] · Germán Arturo Bohórquez Mahecha[3] · Ângela Maria Ribeiro[1,4] · Christopher Kushmerick[1,2,5]

Abstract

Thiamine deficiency is associated with cerebellar dysfunction; however, the consequences of thiamine deficiency on the electrophysiological properties of cerebellar Purkinje cells are poorly understood. Here, we evaluated these parameters in brain slices containing cerebellar vermis. Adult mice were maintained for 12–13 days on a thiamine-free diet coupled with daily injections of pyrithiamine, an inhibitor of thiamine phosphorylation. Morphological analysis revealed a 20% reduction in Purkinje cell and nuclear volume in thiamine-deficient animals compared to feeding-matched controls, with no reduction in cell count. Under whole-cell current clamp, thiamine-deficient Purkinje cells required significantly less current injection to fire an action potential. This reduction in rheobase was not due to a change in voltage threshold. Rather, thiamine-deficient neurons presented significantly higher input resistance specifically in the voltage range just below threshold, which increases their sensitivity to current at these critical membrane potentials. In addition, thiamine deficiency caused a significant decrease in the amplitude of the action potential afterhyperpolarization, broadened the action potential, and decreased the current threshold for depolarization block. When thiamine-deficient animals were allowed to recover for 1 week on a normal diet, rheobase, threshold, action potential half-width, and depolarization block threshold were no longer different from controls. We conclude that thiamine deficiency causes significant but reversible changes to the electrophysiology properties of Purkinje cells prior to pathological morphological alterations or cell loss. Thus, the data obtained in the present study indicate that increased excitability of Purkinje cells may represent a leading indicator of cerebellar dysfunction caused by lack of thiamine.

Keywords Vitamin B_1 · Purkinje neuron · Action potential · Rheobase · Depolarization block

Introduction

This study characterizes changes to the morphology and electrophysiological activity of cerebellar Purkinje cells in mice

✉ Christopher Kushmerick
  kushmerick@ufmg.br

[1] Graduate Program in Neuroscience, Universidade Federal de Minas Gerais, Belo Horizonte, Brazil

[2] Graduate Program in Physiology and Pharmacology, Universidade Federal de Minas Gerais, Belo Horizonte, Brazil

[3] Department of Morphology, Universidade Federal de Minas Gerais, Belo Horizonte, Brazil

[4] Department of Biochemistry and Immunology, Universidade Federal de Minas Gerais, Belo Horizonte, Brazil

[5] Department of Physiology and Biophysics, Universidade Federal de Minas Gerais, Belo Horizonte, Brazil

deprived of thiamine (vitamin B_1) as an animal model for neurological disease caused by thiamine deficiency. The goals of this study are to investigate how thiamine deficiency affects Purkinje cell function and to characterize early events in disease states provoked by thiamine deficiency.

Many previous studies have demonstrated the essential role of thiamine and its metabolites on brain function. The brain is a major consumer of thiamine, and thiamine deficiency causes necrotic lesions in several brain areas [1]. After uptake from the diet, thiamine is phosphorylated to form thiamine monophosphate, diphosphate, and triphosphate. The diphosphate form has well-known roles as a cofactor for metabolic enzymes, and a reduction in thiamine diphosphate is therefore deleterious for all tissues, although certain regions of the brain, including the cerebellum, are particularly susceptible [2]. In addition to its role as a cofactor for metabolic enzymes, thiamine or its phosphorylated derivatives have been shown to modulate ion channels [3, 4]. These observations, together

with the discovery that brain mitochondria synthesize thiamine triphosphate [5], suggest that thiamine phosphates could function as endogenous regulators of neuronal excitability.

In human patients and animal models of human pathologies, thiamine deficiency has been linked to neurodegenerative diseases including Alzheimer's [6–8] and can lead to Wernicke's encephalopathy and Wernicke-Korsakoff syndrome (reviewed by Bubko et al. [9]). Neurological deficit characteristics of these diseases include oculomotor deficits, cognitive dysfunction, memory loss, and ataxia [10–12]. These diseases are characterized by neurodegeneration of several brain regions including thalamus, mammillary bodies, periaqueductal gray matter, inferior and superior colliculus, and cerebellum, mainly in the anterior vermis. Importantly, studies in healthy animals indicate that changes to the temporal pattern of Purkinje cell activity without neurodegeneration reduce the ability to retain information in working memory [13]. This finding indicates the importance of understanding the consequences of thiamine deficiency on the excitability and electrical of individual Purkinje cell. Moreover, the observation that changes to Purkinje cell density and morphology are associated with cognitive decline in Alzheimer's patients [14] highlights the importance of separating effects of thiamine deficiency on Purkinje cell morphology (cell size and cell count) from its effects on intrinsic electrical activity.

In rats, thiamine deficiency can lead to irreversible loss of cerebellar Purkinje cells [15]. Purkinje cells are the sole output neuron from the cerebellar cortex, and therefore, it is important to understand how thiamine deficiency affects these cells culminating in cell death. However, the cellular electrophysiological changes to cerebellar neurons caused by thiamine deficiency are largely unknown. In cultured rat cerebellar granular neurons, treatment with culture media deficient in thiamine caused a decrease in A-type K^+ currents [16, 17] and an increase in CaV1.2 expression and Ca^{2+} current [18]; however, it is unknown if similar changes occur in Purkinje cells. Thiamine deficiency causes marked changes to 5-hydroxytryptamine responses in Purkinje cells [19], consistent with the hypotheses discussed above that thiamine or its derivatives can regulate neuronal excitability. However, since the aforementioned study relied on extracellular recordings, we still do not have any information on the effect of thiamine deficiency on cellular electrical parameters such as input resistance, rheobase, threshold, and AP waveform. Here, we used whole-cell current clamp to measure electrical properties of Purkinje cells from thiamine-deficient animals in brain slices.

An effective treatment to induce thiamine deficiency in rodents consists of a thiamine-free diet combined with daily administration of pyrithiamine [20–22], a thiamine analog that inhibits the enzyme thiamine pyrophosphokinase leading to reduced levels of thiamine diphosphate in the brain [23]. This model produces clinical signs including equilibrium deficits and gait abnormalities [24–27], and recapitulates some of the clinical and neuropathological signs of Wernicke-Korsakoff syndrome observed in human patients including ataxia [28]. Using thiamine-deficient mice as an experimental model, in the present study, we examined changes to Purkinje cell function directly due to thiamine deficiency, before the onset of cell death in the cerebellum.

Methods

Animals and Thiamine Deficiency Model

Experiments were performed on tissue obtained from 33 male C57Bl/6 mice, aged 8–9 weeks at the start of the protocol, obtained from the CEBIO animal facility of the Universidade Federal de Minas Gerais. The justification for including only male subjects was to avoid variability due to estrous cycle. The metabolic pathways for which thiamine diphosphate is a cofactor are very highly conserved, and it is unlikely that significant differences exist between sexes. All protocols and procedures using animals were approved by the local animal care committee (CEUA protocol 71/2018). The experimental schedule is illustrated schematically in Fig. 1a. After a 7-day habituation period, animals were divided randomly into two groups: thiamine-deficient (DEF) and control (CTRL). Thiamine-deficient animals received a thiamine-free diet (Table 1) and received daily injections of pyrithiamine (0.25 mg/kg, i.p.). Control animals were also fed a thiamine-free diet, but received daily injections of thiamine (0.4 mg/kg, i.p.) instead of pyrithiamine. Feeding of control animals was

Table 1　Composition of thiamine-free chow

	g/kg
Cornstarch	507
Cassava starch	169
Casein*	200
Soy oil	50
Salt mixture**	50
Vitamin mixture***	10
Cellulose	10
Choline-HCL	4.0
Tocopherol-vitamin E	0.4
Butylated hydroxytoluene (BHT)	0.1

*Casein was autoclaved before use

**(in %) NaCl (13.93), KI (0.08), $MgSO_4·7H_2O$ (5.73), $CaCO_3$ (38.14), $MnSO_4·H_2O$ (0.40), $FeSO_4·7H_2O$ (2.70), $ZnSO_4·7H_2O$ (0.05), $CuSO_4·5H_2O$ (0.05), $CoCl_2·6H_2O$ (0.02), KH_2PO_4 (38.90)

***(in %) retinyl acetate (0.40), cholecalciferol (0.06), menadione (0.05), myo-inositol (1.00), niacin (0.40), calcium pantothenate (0.40), riboflavin (0.08), pyridoxine-HCl (0.05), folic acid (0.02), biotin (0.004), vitamin B_{12} (0.0003), balance sucrose

restricted to the average daily consumption of the deficient group [25]. This protocol was continued until thiamine-deficient animals presented clinical signs including hunched back and lower limb distension, which occurred on days 12–13. At this time point, matched feeding control animals did not present any clinical alterations.

Upon completion of the thiamine deficiency treatment, groups were further subdivided into animals used for histology ($N = 3$ from each group) or electrophysiology ($N = 7$ CTRL and $N = 6$ DEF). The remaining animals (7 from each group) entered the recovery protocol, which consisted of a single injection of thiamine (1 mg/kg) or water (controls) followed by ad libitum access to standard chow (containing thiamine). After 7-day recovery, these animals were used for electrophysiology. The electrophysiological experiments permitted processing of 1 animal per day. Control animals were analyzed on days 11 and 14, and thiamine-deficient animals on days 12 and 13. Likewise, for recovery, control-recovered animals were analyzed on days 18 and 21, and recovered thiamine-deficient animals on days 19–20.

Preparation of Cerebellar Slices

Mice were anesthetized with isoflurane (89-µg/L air). The anesthetized animal was decapitated, the posterior skull was removed, and the cerebellum was extracted and blocked in the sagittal plane by removing one cerebellar hemisphere with a scalpel cut and mounted with cyanoacrylate glue onto the tray of a Vibratome (Leica VT1000S). The tray was immersed in ice-cold low-Ca^{2+} artificial CSF (aCSF) containing (in mM): 125 NaCl, 25 NaHCO3, 2.5 KCl, 3 MgCl2, 0.1 CaCl2, 25 glucose, 1.25 NaH2PO4, 0.4 ascorbic acid, 3 myo-inositol, 2 Na-pyruvate, and pH 7.4 when bubbled with carbogen (95% O_2, 5% CO_2). Sagittal slices (200 µm) were obtained from the cerebellar vermis in carbogen-bubbled ice-cold low-Ca^{2+} aCSF. After cutting, slices were incubated in carbogen-bubbled normal aCSF (the same composition as low-Ca^{2+} aCSF, except that the concentrations of Ca^{2+} and Mg^{2+} were 2 mM and 1 mM, respectively) at 37 °C for 45 min and subsequently at room temperature (~ 22 °C) and used for recording within 6 h.

Fig. 1 Experimental protocol, feeding, and body weight variations during thiamine deficiency protocol and recovery. a Schematic illustration of the experimental protocol. b Cumulative food consumption during thiamine deficiency treatment. c Body mass during treatment expressed as absolute (C1) or relative to start of treatment (C2)
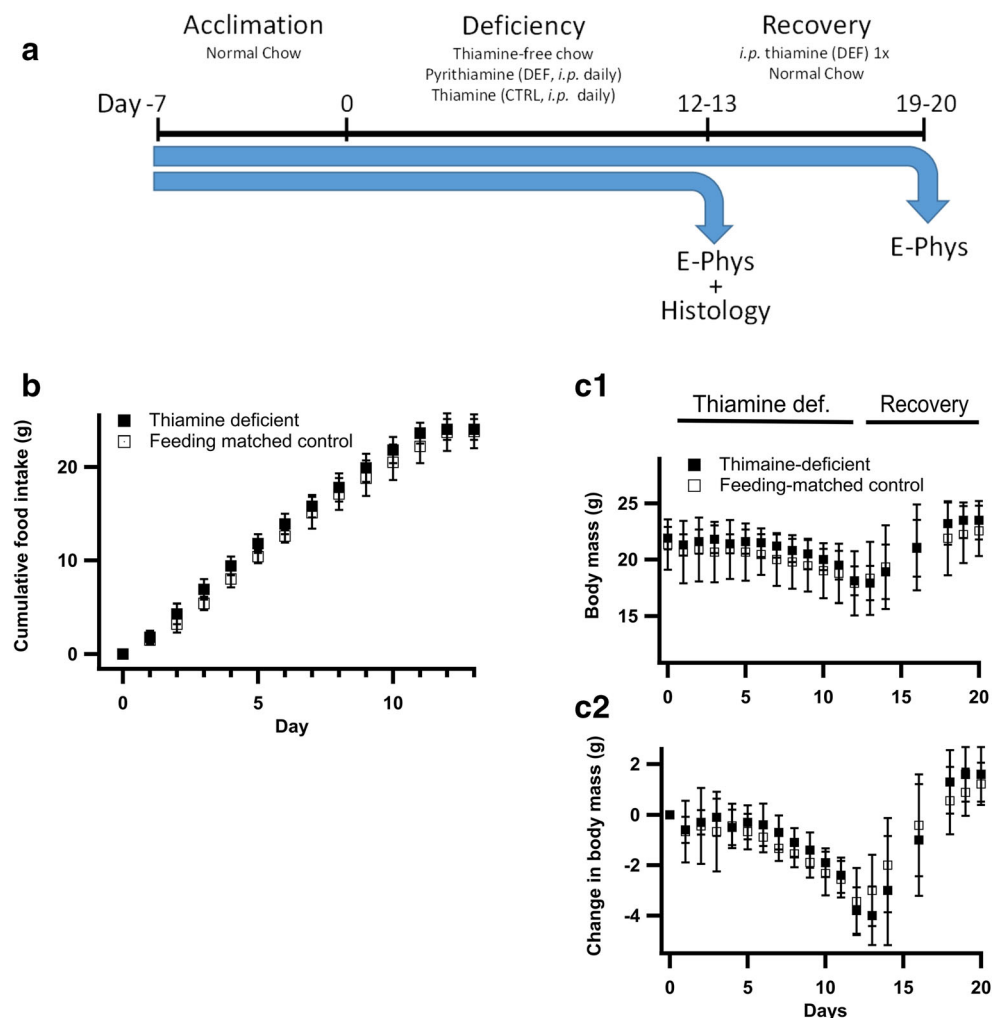
Electrophysiology

Slices were transferred to a 0.5-mL chamber on the stage of a MRK100 microscope (Siskiyou, OR, USA) and kept in place with a platinum harp strung with a nylon thread. The slices were continuously perfused with normal aCSF at a rate of 2 mL/min. Temperature was maintained at 33 ± 1 °C with an inline heater (Warner Instruments model TC-324C). Purkinje cells were visualized with infrared contrast gradient optics through a video camera (IR-1000, DAGE-MTI, IN, USA) and viewed on the monitor of a PC using a video frame grabber and software (ENLTV-FM3, Encore Electronics, USA).

Extracellular and whole-cell current clamp recordings were obtained with an Axopatch 200 amplifier (Axon Instruments, CA, USA). The signals were filtered (low pass, 5 kHz) before being sampled every 24 μs by an A/D converter (Digidata 1322A, Axon Instruments, CA, USA), managed by Strathclyde Electrophysiological Software (created and kindly provided by John Dempster, University of Strathclyde). Pipettes were fabricated from glass capillaries (Patch Clamp Glass, PG52151-4, World Precision Instruments) using a vertical two-stage pipette puller (PP830 Narishige, Tokyo, Japan). Open tip resistance was 2–3 MΩ. Pipettes were coated with dental wax to reduce noise and pipette capacitance. For extracellular recording, pipettes were filled with aCSF, and a juxtacellular recording was made by gently pushing the tip of the pipette < 5 μm into the Purkinje cell soma. For whole-cell recordings, the internal solution contained (in mM): K-gluconate 125, KCl 20, Na2 phosphocreatine 10, EGTA 0.5, HEPES 10, Mg2 ATP 4, Na2 GTP 0.3, pH 7.2 (adjusted with KOH). The calculated liquid junction potential of − 9 mV was corrected online. Data recordings started 5 min after obtaining the whole-cell configuration. From each animal, 1–5 Purkinje cells were recorded.

Using extracellular recordings, we measured spontaneous firing frequency. Under current clamp, the following parameters were evaluated: spontaneous firing frequency, rheobase, input resistance, and the frequency of action potentials as a function of injected current amplitude. For the measurement of spontaneous firing rate, pipette current was set to $I = 0$. For the other measurements, constant current injection was used to maintain the voltage at − 75 mV, and current injection protocols were applied relative to this steady holding current.

Access resistance, R_a, was measured continuously based on the size of the nearly instantaneous jump in pipette potential (ΔV_{inst}) at the onset of a current step (ΔI) as:

$$R_a = \frac{\Delta V_{inst}}{\Delta I} \tag{1}$$

Jumps in pipette potential at the onset of current steps had 10–90% rise time = 0.75 ± 0.15 ms and were thus readily separated from the much slower charging of the membrane capacitance.

Input resistance was measured using hyperpolarizing or depolarizing current injections from a standard Vm = − 75 mV (see above). For hyperpolarizing current injections, negative current injection led to an initial peak hyperpolarization followed by a "sag" (i.e., slow partial repolarization). Peak and steady-state input resistance (R_{in}) was measured from the peak hyperpolarization (ΔV_{peak}) or steady-state hyperpolarization (ΔV_{ss}), and corrected for access resistance (R_a) as:

$$R_{in,peak} = \frac{\Delta V_{peak}}{\Delta I} - R_a \tag{2a}$$

$$R_{in,SS} = \frac{\Delta V_{ss}}{\Delta I} - R_a \tag{2b}$$

Input resistance during subthreshold depolarizing steps was measured by fitting a line to the ΔV vs. ΔI relationship for subthreshold current steps varying in increments of 10 pA. The slope of this line measures the sum of membrane resistance and access resistance, and subthreshold input resistance ($R_{in,subth}$) was calculated by subtracting off the access resistance measured as described above.

$$R_{in,subth} = (\text{Slope of } \Delta V \text{ vs. } \Delta I) - R_a \tag{3}$$

The amplitude of the sag potential was determined as the difference between steady-state membrane potential and peak membrane potentials reached during hyperpolarizing current injections. The time constant of the sag was obtained by fitting a single exponential curve from the negative peak of the hyperpolarization until the end of the current step.

Voltage threshold for action potentials was based on the sudden increase in dVm/dt at the onset of the action potential. Threshold was the membrane potential for which dVm/dt crossed 15 V/s during the upstroke of the action potential. Afterhyperpolarization was measured relative to the voltage threshold [29], and was separate into two kinetic components, fast and slow. Fast afterhyperpolarization was the most negative value of the membrane potential attained during spike repolarization. In our recordings, this occurred < 1 ms after spike peak and decayed with a time constant of about 0.5 ms, giving way to a much slower AHP. The amplitude of the slow AHP was measured after decay (5 time constants) of the fast AHP. Half-width was measured as the width of the AP halfway between threshold and the peak.

To test for spike frequency adaptation, we measured the spike frequency during the first 200 ms ($f_{initial}$) and last 200 ms (f_{final}) of a 1-s current injection, and calculated the adaptation ratio, $f_{final}/f_{initial}$. To measure the minimum current required to cause depolarization block, we applied 1-s current injections in steps of 50 pA from a baseline membrane potential adjusted to − 75 mV using negative bias current. Typically, firing rate increased with increasing current up to certain point and then action potentials began to fail at the end

of the current injection. The amplitude of the last current step for which regular firing occurred throughout the 1-s current injection was taken as the limit for depolarization block.

Only Purkinje cells that had a well-defined membrane and typical cell shape within were chosen for recordings. Access resistance was 17 ± 4 MΩ, and membrane potential was corrected off-line for errors due to series resistance. Cells were excluded from analysis if initial membrane potential, estimated from the intervals between spontaneous spikes, was less negative than -50 mV or if the current required to hold the cells at Vm $= -75$ mV which exceeded -900 pA.

Histology

Animals were sacrificed by overdose with sodium thiopental (5 mg, i.p.) and transcardially perfused with Ringer's solution, followed by Ringer's solution containing glutaraldehyde (2.5%). Cerebellar vermis were embedded in glycol methacrylate (Technovit 7100, Heraeus Kulzer, Wehrheim, Germany), and 3–4-µm serial histological sagittal sections were cut and stained with toluidine blue. To avoid counting the same cell more than one, only each third section was collected. Three animals were used per group. From each animal, 4 sections were collected, and from each section, 5 fields were analyzed resulting in a total of 20 fields per animal, 60 fields per group. Panoramic images from each section were obtained using a Zeiss AxoCam imaging system with a ×4 objective to identify each lobe. High-resolution images containing linear segments of Purkinje layer were taken with a ×40 objective.

Purkinje cell linear density was measured by counting the number of cells in the Purkinje cell layer. Only cells that were aligned with the Purkinje cell layer with well-defined cell plasma membrane were included, resulting in a total of 422 cells counted for control animals and 432 cells counted for thiamine-deficient animals. Cell counts per field were converted to linear density (cell/mm) by dividing by the field length. For cell diameter measurements, in addition to the criteria above, only cells with well-defined nuclear membrane and nucleolus visible in the image were included (131 control cells and 111 thiamine-deficient cells).

Measurements of Purkinje cell major diameter (D1), minor diameter (D2), and nucleus diameter were performed using Image J software (NCBI, Bethesda, USA) by an operator who was unaware of the experimental groupings. Cell and nuclear prolate spheroid areas and ellipsoidal volumes were calculated from their respective major diameters (D1) and minor diameters (D2) as:

$$A = \frac{2 \cdot \pi \cdot D_2^2}{4} \cdot \left(1 + \frac{D_1}{D_2 \cdot \epsilon} \cdot \arcsin \; (\epsilon) \right) \tag{4}$$

$$V = \frac{\pi \cdot D_1 \cdot D_2^2}{6} \tag{5}$$

where ϵ is the eccentricity, $\epsilon = 1 - \frac{D_2^2}{D_1^2}$.

Cell counts and measurements were grouped by regions as anterior (lobes II–V), posterior (lobes VI–IX) or flocular (lobe X). However, because of low cell count for lobe X, it was not considered for statistical analysis.

Chromatin condensation was evaluated from the intensity of nucleus staining using a Nikon Eclipse E600 microscope (Nikon Corp., Melville, USA) with a ×40 objective. Images were converted to a gray scale and inverted using ImageJ software.

Statistics Analysis

Data in figures and text are presented as mean ± standard deviation. Statistical tests were performed using the built-in statistical functions included in Igor 8 (Wavemetrics). Body weight was analyzed by two-way ANOVA for repeated measures. Other parameters were evaluated with Student's t test. Differences were considered statistically significant when $p < 0.05$.

Results

Thiamine Deficiency Reversibly Reduced Feeding and Body Weight

Thiamine deficiency with feeding-matched control was applied using the protocol described in "Methods", and feeding and body mass were monitored daily (Fig. 1). For the first 10 days of the protocol, food intake remained relatively constant. However, on days 11–13, feeding by thiamine-deficient mice was strongly reduced, as observed in previous studies [30], visible as a reduction in the slope of the cumulative feeding curve (Fig. 1b). To control for this effect, we used a matched feeding program whereby food intake of control animals was limited to that consumed by thiamine-deficient animals. Cumulative consumption during the thiamine deficiency protocol was 24.0 ± 1.1 g/animal in the thiamine-deficient group vs. 23.8 ± 1.8 g/animal in control ($p = 0.42$). At the start of treatment, body mass was not statistically different in the control group (21.3 ± 2.2 g) and the thiamine deficiency group (21.1 ± 1.0 g). After treatment, body mass decreased by -3.0 ± 1.4 g (14%) and -4.0 ± 1.2 g (19%), respectively ($p < 0.001$ for the effect of treatment on body mass, $p < 0.05$ for the difference between treatment groups). Thus, both groups lost body mass during treatment, and despite equal feeding, thiamine-deficient animals lost significantly more body mass during treatment although

the difference between groups was small (difference in effect size equal to 5% of original body mass). On days 12–13, thiamine-deficient animals presented clinical signs including hunched back and lower limb distension, whereas in control animals, these clinical signs were absent. In previous studies using the same thiamine deficiency protocol, mice at this stage have other clinical cerebellar signs including difficulty on the rotarod and gait abnormalities [21, 24–27]. Electrophysiological and morphological analyses were thus performed at this time point. Weight loss was completely reversed in both control and thiamine-deficient animals after 7 days recovery.

Thiamine Deficiency Reduced Rheobase of Purkinje Cell Neurons

To determine if thiamine deficiency affects the excitability of cerebellar Purkinje cells, we first measured the rheobase, the current necessary to evoke action potentials (Fig. 2). For these experiments, Purkinje cells were hyperpolarized to a standardized membrane potential of $\cong -75$ mV with steady holding current injection (CTRL, $I_{hold} = -570 \pm 119$ pA vs. DEF, $I_{hold} = -540 \pm 144$ pA, $p = 0.5970$). Under these conditions, spontaneous action potentials were not observed. To measure rheobase, positive current steps of 1-s duration and amplitudes that varied in steps of 10 or 20 pA were applied until the Purkinje cell fired at least one action potential (Fig. 2a). Using this protocol, we observed a marked decrease in minimal current required to fire an action potential in Purkinje cells from thiamine-deficient animals (Fig. 2b, CTRL, rheobase = 460 ± 301 pA vs. DEF, rheobase = 187 ± 119 pA, $p = 0.0012$).

Effects of Thiamine Deficiency on Action Potential Threshold, Waveform, and Afterhyperpolarization

The reduction in rheobase described above for Purkinje cells from thiamine-deficient animals led us to hypothesize a change in action potential threshold. To investigate this, we examined the threshold and kinetics of action potentials to determine if thiamine deficiency affects these parameters (Fig. 3). For this, we employed phase analysis by plotting dVm/dt vs. Vm (Fig. 3a). Action potential maximal rates of depolarization and repolarization were unchanged: maximum rate of depolarization (CTRL: 389 ± 103 V/s vs. DEF: 352 ± 56 V/s, $p = 0.1779$), maximum rate of repolarization (CTRL: -381 ± 80 V/s vs. DEF -389 ± 84 V/s, $p = 0.7922$). Voltage threshold was defined as the membrane potential at which dVm/dt crossed 15 V/s during the rising phase of the action potential. Despite the reduction in rheobase, we observed no significant difference in voltage threshold (V_{th}) in Purkinje cells from thiamine-deficient animals (V_{th}, CTRL: -53.1 ± 5.0 mV vs. DEF: -53.9 ± 5.4 mV, $p = 0.6654$, Fig. 3b). Following an action potential, Purkinje cells displayed a prominent afterhyperpolarization (AHP) that comprised two kinetic components. The fast phase reached a negative peak within 1 ms following the spike peak and decayed with a time constant of about 0.5 ms, giving way to a much slower phase (Fig. 3b). Both fast and slow components of the AHP were significantly reduced in thiamine-deficient Purkinje cells: fast AHP, CTRL: -28 ± 5 mV vs. DEF: -23 ± 5 mV, $p = 0.0034$; slow AHP, CTRL: -9.0 ± 3.3 mV vs. DEF: -6.4 ± 2.8 mV, $p = 0.0096$. We also observed a small (9%) increase in AP half-width in thiamine-deficient Purkinje cells (half-width, CTRL: 0.206 ± 0.016 ms vs. DEF: 0.225 ± 0.027 ms, $p = 0.0080$, Fig. 3b).
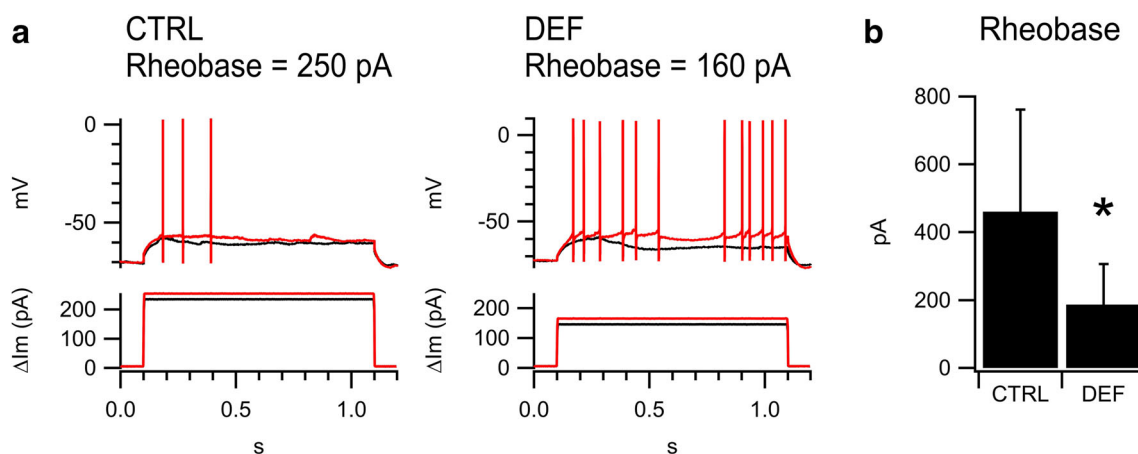
Fig. 2 Thiamine deficiency causes a reduction in rheobase in cerebellar Purkinje cells. **a** Representative recordings from a Purkinje cell from a control (CTRL) or thiamine-deficient (DEF) mouse. Membrane potential was set to $\cong -75$ mV with a constant negative bias current, and current protocols shown are relative to this baseline. Cells were stimulated with step current injections at a resolution of 20 pA. Shown are the last sub-threshold (black traces) and first suprathreshold (red traces) responses. **b** Summary of effect of thiamine deficiency on rheobase (minimum current required to fire an action potential). Error bars represent SD, *$p < 0.05$
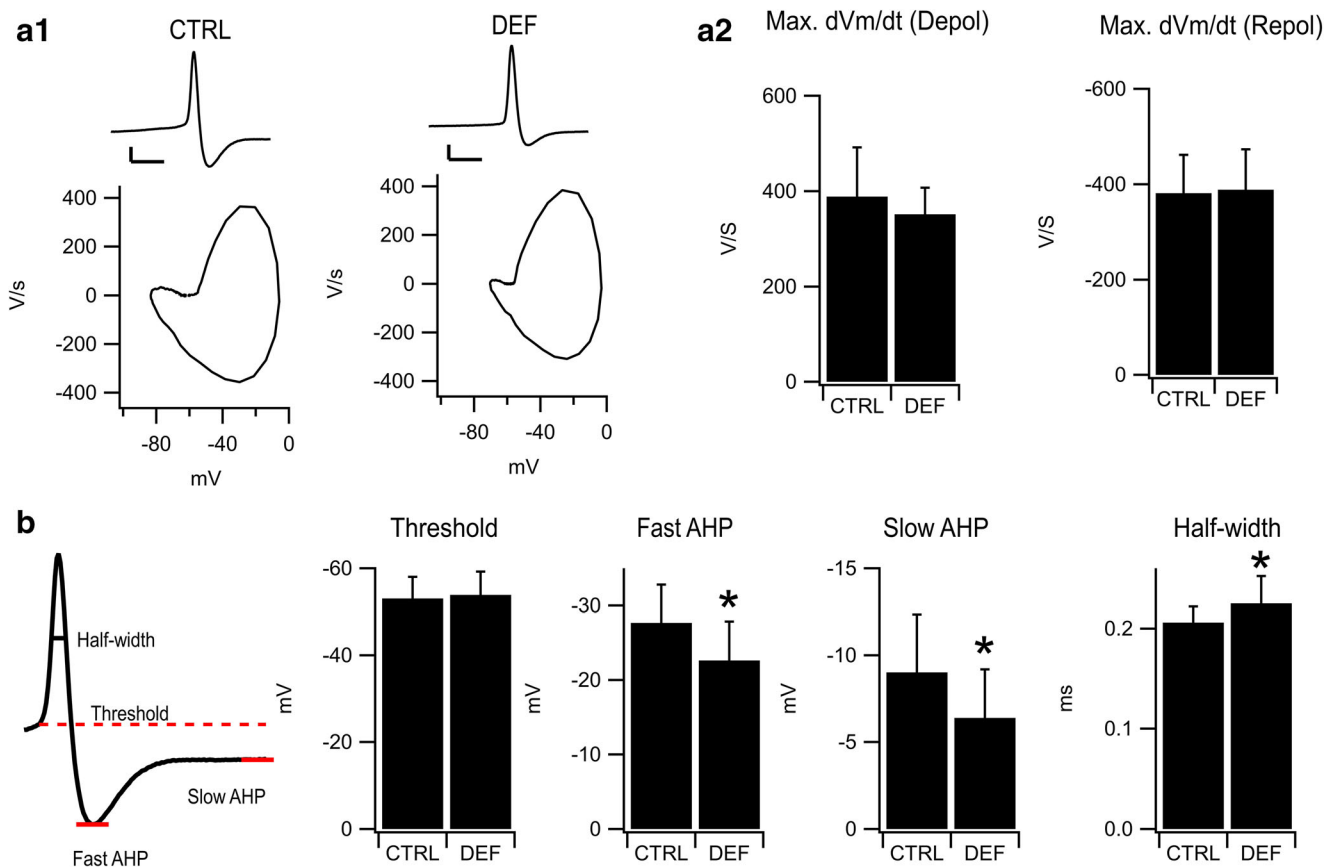
Fig. 3 Changes to the AP waveform in thiamine-deficient Purkinje cells. A1 Action potential and phase-plot analysis of action potential waveform parameters in representative cerebellar Purkinje cells from control (CTRL) or thiamine-deficient (DEF) animals. Cells were hyperpolarized to $\cong -75$ mV and stimulated at their rheobase. Scale bar for inset in **a**: 10 mV, 1 ms. A2 Summary of effects of thiamine deficiency on AP max rate of depolarization and repolarization. **b** Waveform definition and summary of effects of thiamine deficiency on threshold, fast and slow components of the afterhyperpolarization (AHP) and AP half-width. Error bars represent SD, $*p < 0.05$

Thiamine Deficiency Increases Subthreshold Input Resistance

The results described above indicate that voltage threshold was not altered in Purkinje cells from the thiamine-deficient group. We thus considered other possible mechanisms that could explain the observed reduction in rheobase. We analyzed the Purkinje cell input resistance because this parameter determines the amplitude of membrane depolarization produced by a given current injection. Our hypothesis was that higher membrane resistance in thiamine-deficient animals would allow threshold to be reached at lower current intensities than in control.

To test for differences in input resistance, we first measured the voltage response to negative current injection ranging from −200 to −1000 pA (Fig. 4). These stimuli generated hyperpolarizing responses with a prominent depolarizing voltage sag attributable to slow activation of hyperpolarization-activated cyclic nucleotide-gated (HCN) channels [31]. Time to peak hyperpolarization, t_{peak}, was not different between the two groups (CTRL, $t_{peak} = 58 \pm$

13 ms vs. DEF, $t_{peak} = 61 \pm 13$ ms, $p = 0.49$). Dividing the peak change in membrane potential by the amplitude of the current injection and correcting for access resistance (see "Methods," Eq. 2a) gave the peak input resistance, $R_{in,peak}$, which was not different between groups (CTRL, $R_{in,peak} = 26.9 \pm 7.0$ MΩ vs. DEF $R_{in,peak} = 27.4 \pm 5.7$ MΩ, $p = 0.7923$, Fig. 4b). The steady-state input resistance, $R_{in,ss}$, measured at the end of the 1-s current step (Eq. 2b) was also not different between groups (CTRL, $R_{in,ss} = 18.7 \pm 7$ MΩ vs. DEF, $R_{in,ss} = 18.4 \pm 5$ MΩ, $p = 0.8922$, Fig. 4c). We also measured the amplitude and kinetics of the depolarizing voltage sag that followed the initial peak hyperpolarization during negative current injection, as an indirect assessment of HCN conductance. We observed no significant difference in the amplitude of the depolarizing voltage sag (CTRL, $V_{sag} = 7.2 \pm 3.1$ mV vs. DEF, $V_{sag} = 7.9 \pm 2.6$ mV, $p = 0.4255$, Fig. 4d), or its time constant (τ_{sag}, CTRL: 76.5 ± 38 ms vs. DEF: 69 ± 16 ms, $p = 0.3952$, Fig. 4e). Therefore, neither input resistance nor the extent of depolarizing voltage sag during hyperpolarization or its kinetics was significantly different between control and thiamine-deficient animals.

Fig. 4 Membrane responses to − 1 nA hyperpolarizing current injection. **a** Representative responses from Purkinje cells from a control (CTRL) or thiamine-deficient (DEF) mouse. Cells were hyperpolarized to − 75 mV with a constant negative bias current, and current protocol was applied relative to this baseline. **b**–**e** Summary of effects of thiamine deficiency on input resistance, depolarizing voltage sag, and sag time constant. Peak and steady-state input resistance were calculated from the peak and steady-state hyperpolarization after subtracting off the instantaneous jump due to series resistance. Sag depolarization (V_{sag}) was the difference in peak and steady-state depolarization. Sag time constant (τ_{sag}) was determined by adjusting a single exponential curve to the sag depolarization starting at peak hyperpolarization. Error bars represent SD, *$p < 0.05$
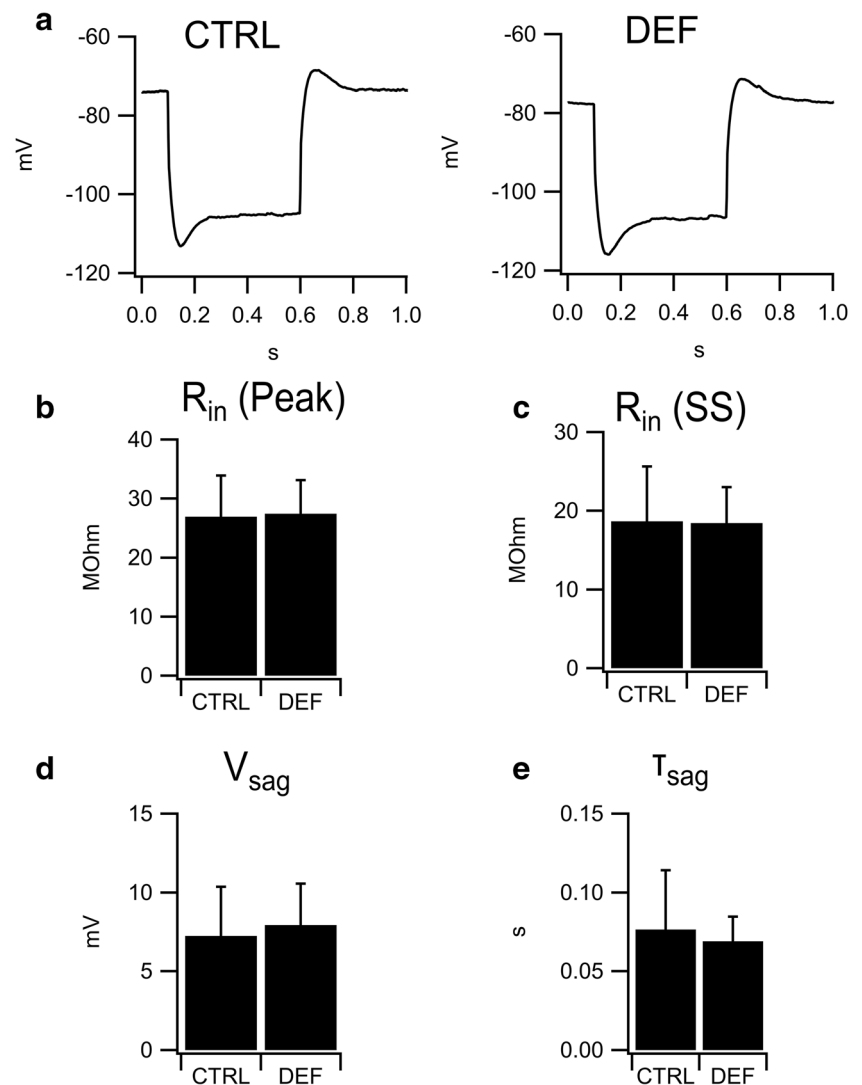
We next examined the behavior of the membrane potential when stimulated with subthreshold-positive current injection (Fig. 5). For these experiments, cells were stimulated with positive current injections that varied in steps of 10 or 20 pA from a membrane potential of − 75 mV. The size of the resultant depolarization was measured as a function of current step, and the input resistance of the membrane was measured at these subthreshold potentials as the slope of the ΔV vs. ΔI relationship ("Methods," Eq. 3, Fig. 5a, b). Using this protocol, we observed a 69% increase in the membrane resistance between thiamine-deficient Purkinje cells and controls measured at these subthreshold potentials, ($R_{in,subth}$, CTRL: 29 ± 18 MΩ vs. DEF: 48 ± 30 MΩ, $p = 0.0158$, Fig. 5c). Higher subthreshold input resistance in thiamine-deficient Purkinje cells explains, at least partially, the reduction in rheobase described above.

Frequency and Variability of Spontaneous and Stimulated Action Potentials

The rate of action potential firing was examined in whole-cell current clamp with no applied current (Fig. 6a). We observed no significant difference in the rate of spontaneous action potentials between groups (CTRL, frequency = 117 ± 48 Hz vs. DEF, frequency = 143 ± 49 Hz, $p = 0.2278$). Since whole-cell perfusion may change the native firing pattern, we repeated these measurements with extracellular recordings (Fig. 6b) and obtained similar results (CTRL, frequency = 122 ± 63 Hz vs. DEF, frequency = 90 ± 29 Hz, $p = 0.4074$). Besides firing rate, another important parameter of Purkinje cell function is temporal dispersion in spike intervals ([32, 33]). We examined this parameter by measuring the coefficient of variation of spike intervals in Purkinje cells spiking at a mean frequency near 100 Hz (CTRL, 109 ± 9 AP/s, DEF, 108 ± 7 AP/s). This analysis indicated that thiamine deficiency did not change the

a

CTRL

b

DEF

CTRL (Avg)

DEF (Avg)

c

Slope R$_{in}$
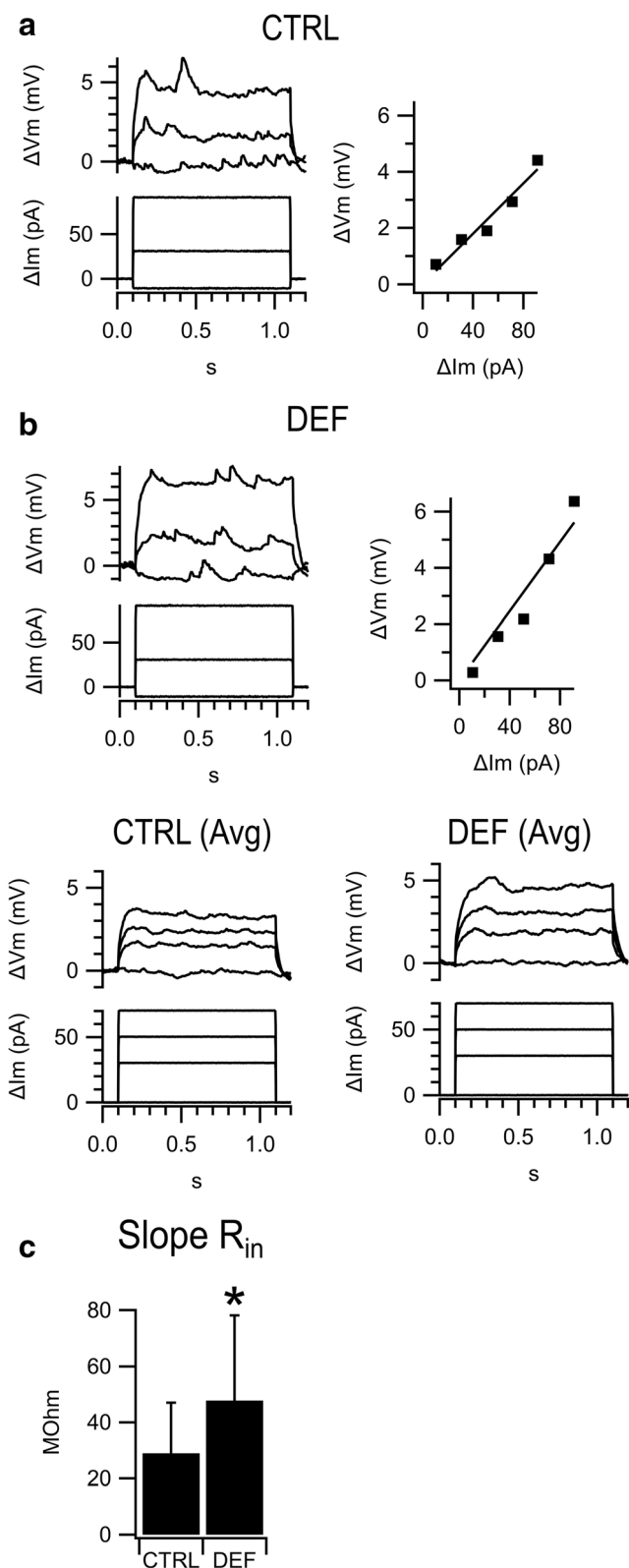
◀ **Fig. 5** Subthreshold input resistance is significantly increased in Purkinje cells from thiamine-deficient animals. Cells were hyperpolarized to − 75 mV, and current injections were applied to measure the input resistance at subthreshold membrane potential. **a** Voltage responses to small hyperpolarizing and depolarizing current injections, and V–I plot used to determine Rin for a representative control Purkinje cell. **b** The same as for **a**, except for a Purkinje cell from a thiamine-deficient animal. **c** Summary of difference in slope input resistance for the two groups. Error bars represent SD, *$p < 0.05$

We next examined the firing of Purkinje cells when stimulated with current injections above their rheobase and determined the gain of the input/output relationship as the slope of the frequency vs. current relationship. These data indicate no significant difference in input/output gain in thiamine-deficient animals compared to controls (CTRL, slope = 0.55 ± 0.12 AP/s/pA vs. DEF, slope = 0.53 ± 0.050 AP/s/pA, $p = 0.87$) (Fig. 6d, e). To determine if spike frequency adaptation occurred during the 1-s depolarizing current injection, we calculated the spike frequency adaptation ratio, $f_{\text{final}}/f_{\text{initial}}$ (see "Methods"). Although there was significant dispersion during current levels just above rheobase, for stronger current injection $f_{\text{final}}/f_{\text{initial}}$ converged to a value slightly greater than 1.0 (slightly greater firing at the end of the current injection) for both the CTRL and DEF groups with no significant difference between groups (Fig. 6f, g).

To determine if thiamine-deficient Purkinje cells were more sensitive to depolarization block [34], we applied current injections in steps of 50 pA and determined the level of current for which action potentials failed during the 1-s current application (Fig. 6h–j). Thiamine-deficient cells required significantly less current for depolarization block than controls (CTRL, 1.71 ± 0.21 nA vs. DEF, 1.17 ± 0.47 nA, $p = 0.003$, Fig. 6i). Thiamine-deficient cells also entered depolarization block at a lower spike rate compared to controls, although this difference was not statistically significant (CTRL, 394 ± 139 spikes/s vs DEF, 309 ± 84 spikes/s, $p = 0.0845$, Fig. 6j).

To determine the overall cellular health of the Purkinje cell layer in thiamine-deficient mice, we measured the cell density and cell size of Purkinje cells in cerebella from deficient and control animals (Fig. 7). Randomly chosen fields containing the Purkinje cell layer showed no difference in the number of cells between control and thiamine-deficient animals (CTRL, 23.4 ± 6.2 cells/mm vs. DEF, 24.0 ± 6.7 cells/mm, $p = 0.78$), (Fig. 7b). Thus, thiamine deficiency did not cause a reduction in the total number of Purkinje cells. We next examined the size of the Purkinje cells and observed a significant reduction in the volume of Purkinje cell soma from thiamine-deficient animals (CTRL, soma volume = 2.8 ± 0.76 pL vs. DEF, soma volume 2.3 ± 0.79 pL, $p < 10^{-4}$), (Fig. 7c). To look for signs of apoptosis, we examined the cell nuclei. No increase in the density of staining of nuclei was observed (not shown). We did detect a decrease in nuclear volume (Fig. 7d); however, this decrease was in proportion to the somatic volume change.

regularity of Purkinje cell spiking (CTRL, CV = 0.18 ± 0.17 vs. DEF, CV = 0.16 ± 0.12, $p = 0.7767$, Fig. 6c).
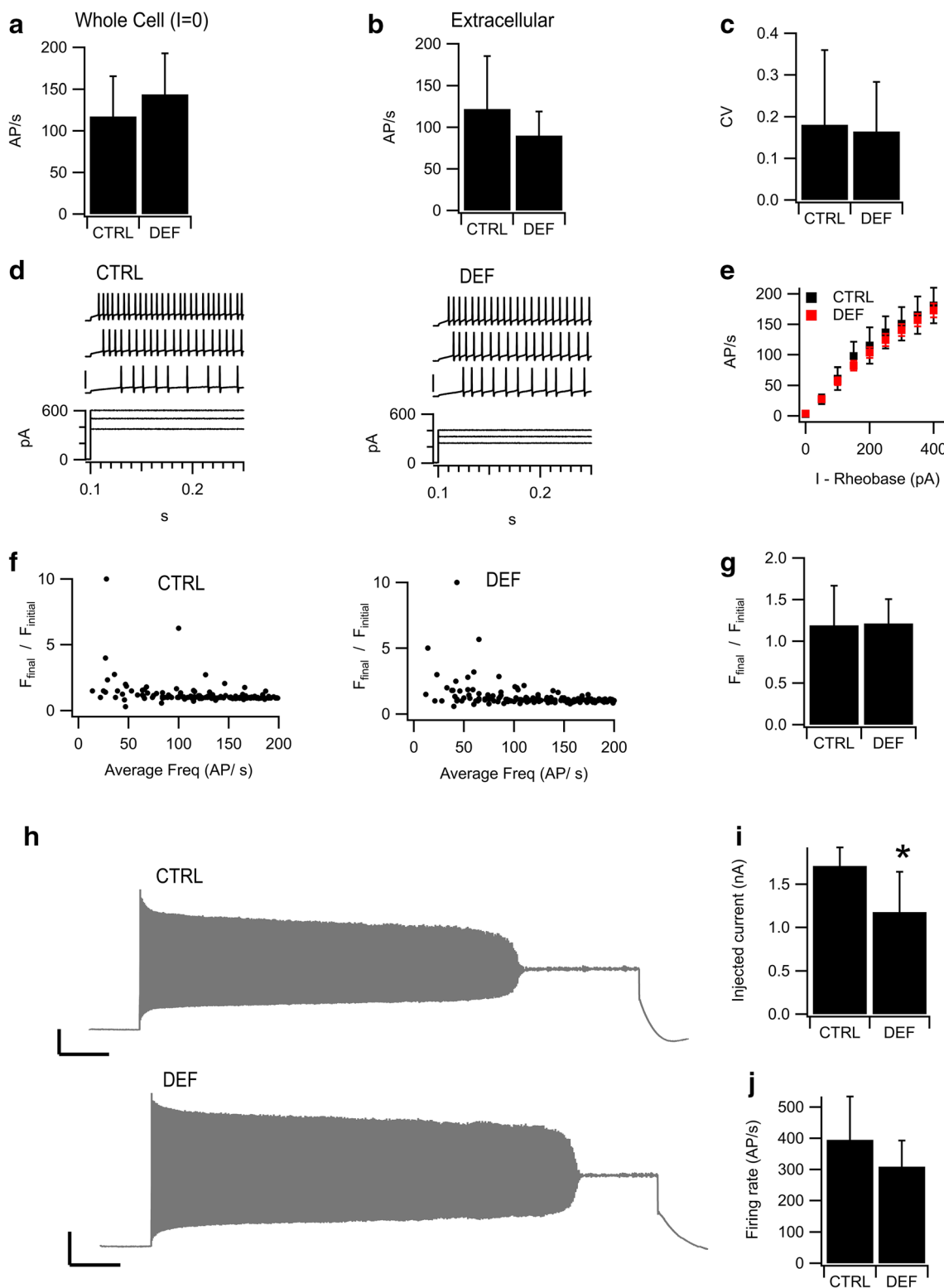
Fig. 6 Spontaneous and stimulated action potential frequency. **a** Spontaneous action potential frequency in whole-cell recordings ($I = 0$). **b** Spontaneous action potential frequency for extracellular recordings. **c** Coefficient of variation of inter-spike intervals in whole-cell recordings. **d** Responses to Purkinje cells from control or thiamine-deficient animals when stimulated at 1×, 1.5×, and 2× rheobase. Scale bar, 50 mV. **e** Input/ output relationship, normalized to rheobase, for the two groups. **f** All-cell plot of accommodation index as a function of average firing rate for cells stimulated above their rheobase. **g** Summary of accommodation at an average firing rate of 90 AP/s. **h** Representative traces of control and deficient Purkinje cells stimulated with current that generates depolarization block. Scale bars, 0.1 s and 20 mV. **i** Summary of the current required to generate depolarization block. **j** Summary of the firing rate at which depolarization block occurred. Error bars represent SD, $*p < 0.05$
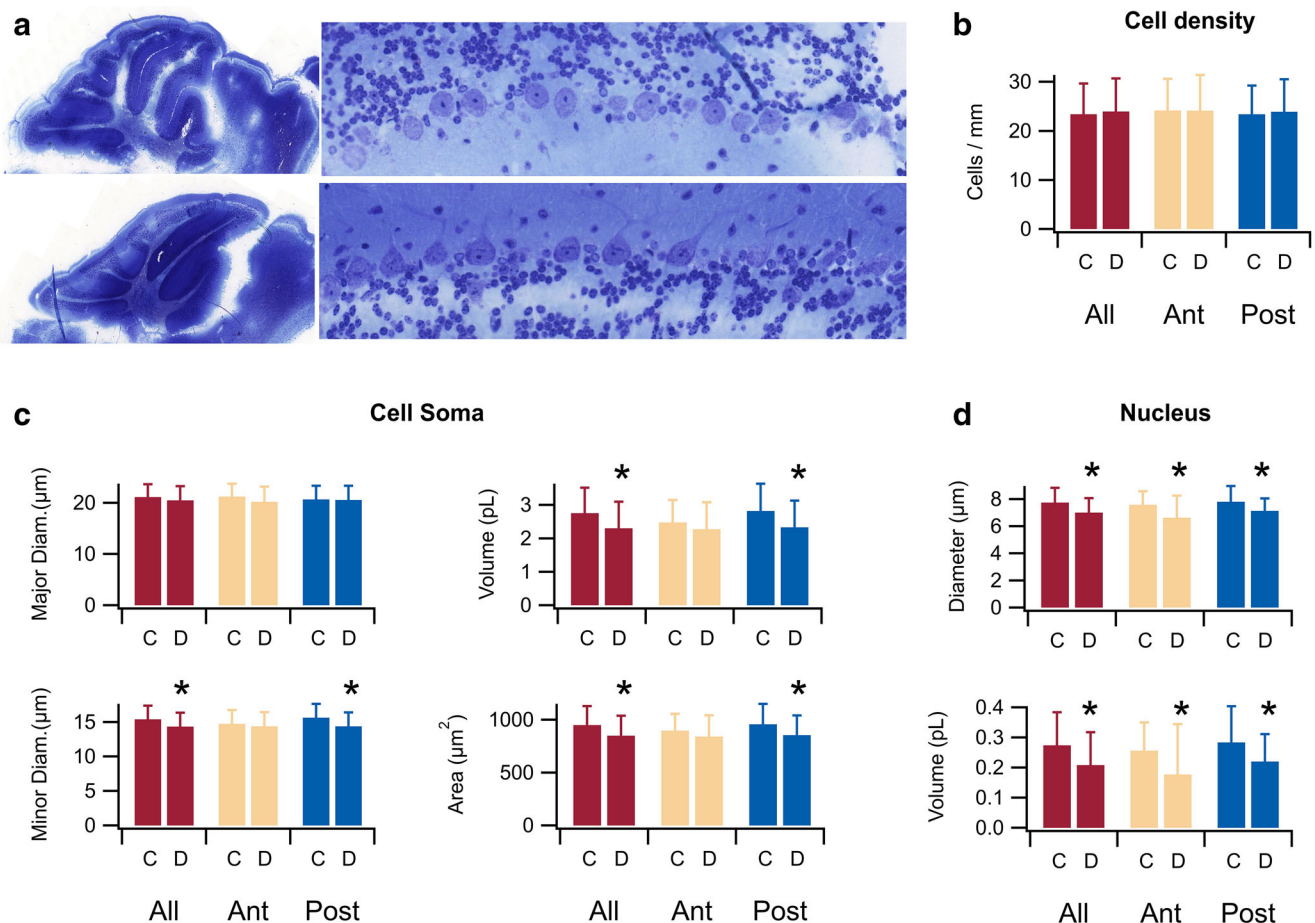
Fig. 7 Thiamine deficiency reduces Purkinje cell and nuclear volume, with no reduction in cell number. **a** Panoramic and high-magnification images of sections of cerebella from a control mouse (upper panels) or thiamine-deficient mouse (lower panels). Scale bars are 500 μm and 50 μm. **b** Purkinje cell density. **c** Measured major diameter and minor diameter of Purkinje cell soma and calculated surface area and volume. **d** Measured diameter and calculated volume of Purkinje cell nucleus. C control cells, D thiamine-deficient cells. Error bars represent SD, *$p < 0.05$

Thus, we did not detect any of the hallmarks of apoptosis such as nuclear condensation or fragmentation. Therefore, the thiamine deficiency protocol we used does not appear to cause overt degeneration of the Purkinje cell layer at the time point studied.

The results above indicate that thiamine deficiency protocol employed reduced the rheobase current and the afterhyperpolarization, without inducing significant cell death. This raises the possibility that treatment of thiamine-deficient animals with thiamine might restore normal Purkinje cell function. To test this, animals were subjected to the thiamine deficiency protocol (or feeding-matched control protocol) followed by the recovery protocol described in "Methods." After 7-day recovery, animal weight was completely restored (Fig. 1). Electrophysiological measurements indicated no significant difference in the rheobase, afterhyperpolarization, or half-width for Purkinje cells from thiamine-deficient recovered animals and their corresponding controls (Fig. 8, CTRL, rheobase = 280 ± 187 pA vs. DEF,

rheobase = 291 ± 192 pA, $p = 0.79$; fast AHP = − 26.2 ± 6.3 mV vs. − 25.9 ± 5.4 mV, $p = 0.86$; slow AHP = − 9.0 ± 4.1 mV vs. − 9.3 ± 3.9 mV $p = 0.83$; half-width = 0.212 ± 0.029 ms vs. 0.223 ± 0.039, $p = 0.28$). Thus, the electrophysiological changes caused by thiamine deficiency were completely restored after the 7-day recovery.

Discussion

The results presented demonstrate that thiamine deficiency reduces the rheobase for simple spike firing in Purkinje cells and reduces both fast and slow components of the afterhyperpolarization following simple spikes, with a modest broadening of the AP. In addition, thiamine-deficient Purkinje cells required less current to enter depolarization block. These electrophysiological changes were accompanied by an increase in input resistance detected during subthreshold depolarizing current injections. Histological analysis revealed

Fig. 8 No difference in rheobase of Purkinje cells from control-recovered (CTRL) and thiamine-deficient-recovered (DEF) mice. Animals were subjected to the thiamine deficiency protocol (or feeding-matched control protocol) for 12 days, followed by the recovery protocol for 7 days. Error bars represent SD

After recovery protocol
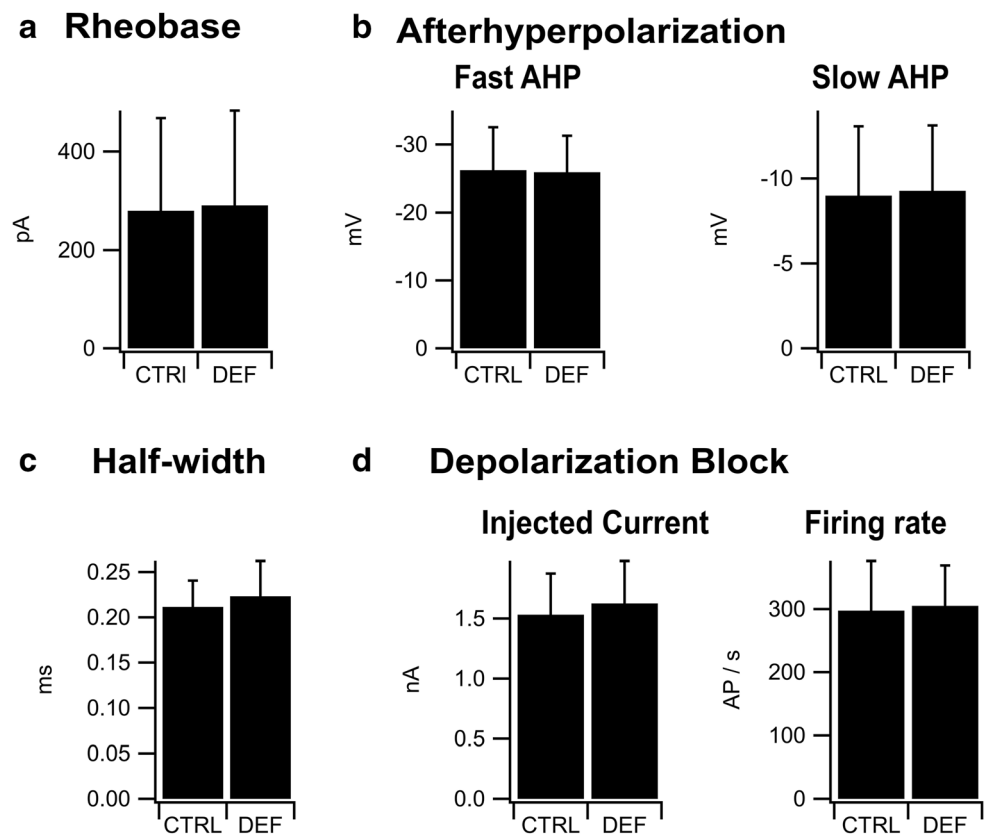
a small reduction in Purkinje cell volume but no reduction in cell count, indicating little or no overt Purkinje cell deterioration or death. Consistent with this, the electrophysiological alterations described above were completely absent in Purkinje cells from mice that completed the recovery protocol after thiamine deficiency.

Purkinje cells generate complex electrical activity consisting of both fast somatic sodium spikes mediated by TTX-sensitive Na^+ channels and slower dendritic Ca^{2+} spikes mediated by P-type Ca^{2+} currents (reviewed by Llinás [35]). In addition to providing regenerative drive for Ca^{2+} spikes, Ca^{2+} entry through voltage-gated Ca^{2+} channels also couples to the activation of BK and SK type Ca^{2+}-sensitive K^+ channels present in the soma and dendrites [36–42]. Inhibition of BK channels with iberiotoxin or SK channels with apamin reduces the afterhyperpolarization following each action potential [29, 43]. Conversely, EBIO, an activator of SK channels, increases the afterhyperpolarization [38]. In addition to Ca^{2+}-dependent potassium channels, Purkinje cells also express 4-AP-sensitive A-type potassium currents [44] which are required for the dendritic afterhyperpolarization that follows subthreshold current injection, reviewed by Schreurs [45].

It thus appears that BK and SK Ca^{2+}-dependent K channels and A-type K channels can contribute to the I_{AHP} that underlie afterhyperpolarizations in Purkinje cells. Block of BK channels with iberiotoxin [29, 36, 42] or A-type potassium channels with 4-AP [36, 44] produces changes to simple spike waveform similar to what we observed in thiamine-deficient Purkinje cells, although thiamine deficiency caused less broadening of the action potential than 4-AP (9% increase in half-width by thiamine deficiency compared to 61% increase in half-width by 4-AP, Table 1 in Belmeguenai et al. [36]). Thus, we consider BK channels and A-type potassium channels as possible mediators of the effects of thiamine deficiency on AP waveform.

Downregulation of SK type Ca^{2+}-sensitive potassium channels is associated with increased excitability in Purkinje cells [36, 46], but for reasons described below, we think it is unlikely that a reduction in SK channel density would explain the effects of thiamine deficiency on Purkinje cell excitability. First, because thiamine deficiency did not change, either spontaneous firing rate or the slope of the relationship between firing rate and injected current as would be expected based on previous studies in which SK channels was blocked with apamin or downregulated [29,

47]. Second, the reduction in input resistance in thiamine-deficient Purkinje cells was only observed for subthreshold depolarizations and was not observed during hyperpolarizing current injections. This asymmetry implies the involvement of a voltage-gated channel controlling input resistance, and SK channels are not voltage-sensitive (reviewed by Adelman et al. [48]). Third, whereas thiamine deficiency increased subthreshold input resistance, intrinsic excitability plasticity in Purkinje cells known to be dependent on SK channel downregulation is not associated with a change in input resistance [36].

Slow afterhyperpolarizations can regulate the inter-spike interval and thus determine the pace of spontaneously firing neurons. However, we observed a reduction in afterhyperpolarization in thiamine-deficient Purkinje cells without a concomitant increase in firing rate. In our whole-cell recordings from control animals, spontaneous firing rate in many cells was above 100 spikes per second, a result that was verified using less-invasive juxtacellular recordings. This rate of firing is high for adult mouse Purkinje cells [49]. We note that our recordings were from the anterior zone (nodes III–V) where firing rates tend to be higher at least in part due to a higher percentage of Zebrin-negative cells [47, 49–51]. It is possible that this high rate of spontaneous firing occluded a potential further increase due to the reduced afterhyperpolarization in thiamine-deficient cells. We also note that changes in firing rate do not always correlate well with changes to the size of the afterhyperpolarization. For example, inhibition of BK channels with iberiotoxin produced a strong decrease in afterhyperpolarization and a modest increase in firing rate compared to SK which produced a strong increase in firing rate with little inhibition of the AHP [29]. Moreover, Purkinje cells from BK-knockout mice that have smaller afterhyperpolarization fired at a lower rate than wild-type controls [42]. Similarly, corticotropin-releasing factor reduced the afterhyperpolarization without causing a significant effect on firing rate [52]. Thus, the relationship between afterhyperpolarization and firing rate does not appear to be direct or simple.

Changes similar to what we describe for thiamine deficiency (increased excitability, reduced afterhyperpolarization) also occur during physiological neuronal plasticity that underlies cerebellar motor learning [36, 45]. This raises the question of whether the effects we observed are a direct consequence of lack of thiamine on Purkinje cell function, that is, a "biochemical lesion" [53] or a compensatory response, perhaps related to intrinsic plasticity during cerebellar motor learning. One difference relates to spatial specificity. Changes to excitability after eyeblink conditioning are localized to Purkinje cells in lobule HVI, the pertinent area of the cerebellum defined by ablation studies as reviewed by Schreurs [45]. In contrast, we observed changes to excitability throughout anterior lobes III–V. A second difference relates to the mechanism, which

appears to be different because intrinsic excitability plasticity depends on downregulation of SK2 channels [54, 55] whereas the effects of thiamine do not appear to be mediated by SK channels for reasons given above. The effects of thiamine deficiency resemble in some ways those observed in Purkinje cells from SCA3 mice, a model of spinocerebellar ataxia type 3, which, like thiamine-deficient Purkinje cells, have a reduced threshold for depolarization block [34]. Although the defect identified in SCA3 mice was related to inactivation of a voltage-activated K channel, normal firing properties could be rescued with an activator of SK channels [34]. This finding supports the idea that SK channels are important regulators of Purkinje cell excitability and potential therapeutic targets even when the primary alteration is not directly related to expression of these channels. Future experiments might test SK channel activators on the excitability of thiamine-deficient Purkinje cell neurons to determine if they can restore normal rheobase and depolarization block threshold.

The effect of thiamine deficiency on Purkinje cell electrophysiological properties is similar to results obtained in cerebellar granular cells maintained in thiamine-deficient media [16, 18], which exhibited a reduction in A-type K^+ current and for which model calculations predicted lower threshold conductance for synaptic inputs. Due to overlap of activation and inactivation voltage dependence, A-type K^+ channels in cerebellar Purkinje cells can produce significant window current [56]. It is therefore possible that thiamine deficiency affects subthreshold membrane resistance and rheobase through a reduction in A-type K channel activity. Dysregulation of K^+ channels may provide a link between the early electrophysiological observations we observe and neuronal cell death from severe thiamine deficiency as modulation of A-type K^+ channels can drive cells to apoptosis [57] and may be involved in ethanol-induced cell loss [58, 59].

Thiamine diphosphate is an essential cofactor for enzymes that mediate oxidative phosphorylation via the Krebs cycle and nucleotide synthesis [60]. As such, systemic deficiency of thiamine is expected to adversely affect essentially all cells in the body. Nonetheless, some organs appear more sensitive to lack of thiamine, and these include the cerebellum [2]. Considering its well-known roles in motor control, equilibrium, and memory, the high sensitivity of the cerebellum to decreased thiamine likely contributes to clinical signs and symptoms of thiamine deficiency that include ataxias, nystagmus, and cognitive deficits [10, 11].

Many different experimental models have been used to study the effects of thiamine deficiency on the nervous system. These include both in vivo and in vitro preparations [12, 18–20]. These models recapitulate many aspects observed in human patients, including the sensitivity of the cerebellum to reduced thiamine [27]. Paradoxically, the rat brain as a whole appears to receive a privileged share of total thiamine as brains

from rats maintained on a very low thiamine diet maintained much higher activity of transketolase (a thiamine diphosphate–dependent enzyme) and levels of thiamine diphosphate compared to other organs [61, 62]. The mechanism responsible for this protection is unknown, although differential expression of thiamine transporter was ruled out. Regardless of the mechanism, it can be overcome by treatment with pyrithiamine which effectively lowers levels of thiamine and its derivatives in the brain [23].

Here, the thiamine deficiency model used was a thiamine-free diet associated with daily injections of pyrithiamine. After 12–13-day treatment, animals in the thiamine-deficient group exhibited clinical signs of mild-stage thiamine deficiency such as decreased appetite, lower limb distension, and hunching [28, 63]. Thiamine deficiency induced with this protocol also produces loss of equilibrium and gait abnormalities as evaluated by changes to paw print patterns and reduced performance on the rotarod [21, 25, 26]. Control animals were restricted to the same level of food intake but did not develop postural signs. During the deficiency treatment, thiamine-deficient animals exhibited reduced feeding as previously reported [30]. To reduce this confounding factor and to study effects specifically related to thiamine deficiency and not general nutritional status, we restricted feeding of controls to that of the thiamine-deficient group. Under this protocol, both groups lost weight, and the difference in weight loss in thiamine-deficient animals compared to controls was relatively small (19% vs. 14%).

Many studies have examined changes to cerebellar structure and function in patients with thiamine insufficiency. In many cases, the patients studied also suffered from alcoholism, which is a major cause of thiamine deficiency in the developed world. But thiamine deficiency can also result from generalized malnutrition, especially in developing or underprivileged populations [64, 65] and in patients with poor intestinal absorption [66]. The presence of confounding factors such as alcoholism or other diseases makes generalizations difficult, but one important clinical distinction is cases for which treatment with thiamine alleviates clinical signs and symptoms and cases for which thiamine deficiency leads to long-term sequela despite treatment. The latter case can occur in either severe prolonged thiamine deficiency in adults [67] or thiamine deficiency during the development of the nervous system in neonatal patients or experimental animal models [12, 68]. In these cases, permanent damage is likely caused by irreversible neuronal death, or persistent changes to protein expression [67, 69]. The sequence of events that occur during thiamine deficiency resulting in permanent damage to the cerebellum is poorly understood. Here, we utilized an experimental model of thiamine deficiency in mice that produced moderate symptoms including reduced feeding and postural alterations. Our goal was to understand the changes to electrophysiological properties of cerebellar Purkinje cells during the early stages of thiamine deficiency.

In some regards, the electrophysiological properties of thiamine-deficient Purkinje cells were similar to controls. Both groups fired action potentials either spontaneously or in response to current injection following a previous hyperpolarization. The action potential afterhyperpolarization was significantly smaller in neurons from thiamine-deficient animals, but other parameters such as voltage threshold and the maximum rate of voltage change during the upstroke or downstroke of the action potential were not different between groups. These data suggest little or no change to expression of the voltage-dependent Na^+ and K^+ channels responsible for depolarization and repolarization phases of the action potential.

However, thiamine deficiency caused a marked decrease in rheobase, a parameter that measures the amount of current required to generate an action potential. These measurements were made from a standardized resting potential of -75 mV, and therefore, these cannot be explained by different levels of baseline membrane potential. The difference caused by alterations in voltage threshold, which, as discussed above, was not different between groups. Rather, we determined that the decrease in threshold was due to an increase in cellular input resistance. Input resistance measures the impact of a given current injection on membrane potential and directly affects the efficiency of synaptic inputs. Interestingly, in thiamine-deficient Purkinje cells, increased input resistance occurred specifically in the subthreshold region of membrane potential. Input resistance increased when the membrane was depolarized towards threshold, but not during hyperpolarizations for which the passive responses and depolarizing sag were unchanged by thiamine deficiency.

Cerebellar Purkinje cells are part of a complex circuit that integrates information from many sources and provides the sole output from the cerebellar cortex. Like other neuronal types, the activity of Purkinje cells is regulated by its synaptic inputs, which include excitatory inputs from parallel fibers and climbing fibers and inhibition by GABAergic basket cells and stellate cells. The impact of these synaptic inputs depends on the intrinsic properties of the post-synaptic neuron. In this context, an increase in input resistance such as we describe for thiamine-deficient Purkinje cells is predicted to increase the impact of a given current. For the case of current clamp injections, the result is a lower rheobase required to achieve the membrane potential threshold for firing. For synaptic currents, high R_{in} will affect the size of synaptic potentials and if the increase in input resistance affects the membrane time constant significantly, it may also affect synaptic integration. Recording from mouse Purkinje cells in vivo demonstrates hyperpolarizing after potentials following climbing fiber–evoked complex spikes [70]. These events bring membrane potential into the subthreshold

voltage range for which we observed an increase in membrane resistance. It thus seems possible that the effect of thiamine deficiency will affect the function of the Purkinje cells.

Histological analysis did not detect a reduction in the number of Purkinje cells in cerebella from thiamine-deficient animals. We did, however, determine a significant reduction in Purkinje cell soma and nuclear volumes, on the order of 20%. These results are reminiscent of studies of brains from alcoholic patients with moderate clinical signs of thiamine deficiency [10, 67] or in rats with ataxia following acrylamide poisoning [71] for which there was no significant reduction in cell number although cell volume was reduced. In our experiments, the smaller Purkinje cell volume corresponds to a reduction of soma membrane surface area by about 16%. It is expected that input resistance would increase with a reduction in cell size provided all other factors remain equal, especially ion channel density. Nonetheless, it is unlikely that the morphological changes can explain directly the electrophysiological alterations observed, for two reasons. Firstly, because of the discrepancy in the magnitude of the effects (16% reduction in cell soma membrane area vs. 80% increase in input resistance, although we note that our histology did not quantify the dendritic arbor). Secondly, the observed increase in input resistance occurred within a very narrow voltage range just below threshold, which cannot be explained by a generalized effect of cell size. Rather, it is far more likely that thiamine deficiency leads to a change in the expression of specific ion channels that are active within this voltage range.

Severe human diseases associated with thiamine deficiency, notably Wernicke-Korsakoff syndrome, can produce cell death in the cerebellum [67]. Malnutrition is common in severe alcoholism, which can lead directly to thiamine insufficiency. In addition, ethanol inhibits the pyrophosphorylation of thiamine to thiamine diphosphate, further reducing supply of this essential cofactor [72]. Reduced activity of enzymes for oxidative glycolysis leads to reduced ATP [73] altered cellular homeostasis [72]. It is still unclear why, among brain regions, the cerebellum is particularly susceptible to reduced thiamine dietary uptake or poor utilization. Turnover of thiamine by cerebellum is high among brain regions [2], as is expression of thiamine pyrophosphokinase [74]. The high rate of utilization of thiamine by the cerebellum may make it particularly sensitive to disruption of supply. Together with the fact that the electrophysiological changes caused by thiamine deficiency could be completely reversed with the recovery protocol suggests that early detection in patients with thiamine deficiency, before irreversible cell death occurs, could improve prognosis.

Compliance with Ethical Standards

Conflict of Interest The authors declare that they have no conflict of interest.

References

1. Hazell AS, Butterworth RF. Update of cell damage mechanisms in thiamine deficiency: focus on oxidative stress, excitotoxicity and inflammation. Alcohol Alcohol. 2009;44(2):141–7.

2. Mulholland P. Susceptibility of the cerebellum to thiamine deficiency. Cerebellum. 2006;5(1):55–63.

3. Bettendorff L, Kolb HA, Schoffeniels E. Thiamine triphosphate activates an anion channel of large unit conductance in neuroblastoma cells. J Membr Biol. 1993;136(3):281–8.

4. Houzen H, Kanno M. Thiamine and its derivatives inhibit delayed rectifier potassium channels of rat cultured cortical neurons. Neuropharmacology. 1998;37(3):313–22.

5. Gangolf M, Wins P, Thiry M, El Moualij B, Bettendorff L. Thiamine triphosphate synthesis in rat brain occurs in mitochondria and is coupled to the respiratory chain. J Biol Chem. 2010;285(1):583–94.

6. Mastrogiacomo F, Bettendorff L, Grisar T, Kish SJ. Brain thiamine, its phosphate esters, and its metabolizing enzymes in Alzheimer's disease. Ann Neurol. 1996;39(5):585–91.

7. Vinh Quc Lu'O'Ng K, Nguyen LTH. Role of thiamine in Alzheimer's disease. Am J Alzheimers Dis Other Dement. 2011;26(8):588–98.

8. Yu Q, Liu H, Sang S, Chen L, Zhao Y, Wang Y, et al. Thiamine deficiency contributes to synapse and neural circuit defects. Biol Res. 2018;51(1):1–9.

9. Bubko I, Gruber BM, Anuszewska EL. The role of thiamine in neurodegenerative diseases. Postepy Higieny i Medycyny Doswiadczalnej (Online). 2015;69:1096–106.

10. Andersen BB. Reduction of Purkinje cell volume in cerebellum of alcoholics. Brain Res. 2004;1007(1–2):10–8.

11. Butterworth RF. Cerebral thiamine-dependent enzyme changes in experimental Wernicke's encephalopathy. Metab Brain Dis. 1986;1(3):165–75.

12. Ferreira-Vieira TH, de Freitas-Silva DM, Ribeiro AF, Pereira SRC, Ribeiro ÂM. Perinatal thiamine restriction affects central GABA and glutamate concentrations and motor behavior of adult rat offspring. Neurosci Lett. 2016;617:182–7.

13. Deverett B, Kislin M, Tank DW, Wang SSH. Cerebellar disruption impairs working memory during evidence accumulation. Nat Commun. 2019;10(1):1–7.

14. Mavroudis I, Petridis F, Kazis D, Njau SN, Costa V, Baloyannis SJ. Purkinje cells pathology in Alzheimer's disease. Am J Alzheimers Dis Other Dement. 2019;34(7–8):439–49.

15. Irle E, Markowitsch HJ. Widespread neuroanatomical damage and learning deficits following chronic alcohol consumption or

vitamin-B1 (thiamine) deficiency in rats. Behav Brain Res. 1983;9(3):277–94.

16. Cruz JS, Kushmerick C, Moreira-Lobo DC, Oliveira FA. Thiamine deficiency in vitro accelerates A-type potassium current inactivation in cerebellar granule neurons. Neuroscience. 2012;221:108–14.

17. Oliveira FA, Galan DT, Ribeiro AM, Cruz JS. Thiamine deficiency during pregnancy leads to cerebellar neuronal death in rat offspring: role of voltage-dependent K+ channels. Brain Res. 2007;1134:79–86.

18. Moreira-Lobo DC, Cruz JS, Silva FR, Ribeiro FM, Kushmerick C, Oliveira FA. Thiamine deficiency increases Ca2+ current and CaV1.2 L-type Ca2+ channel levels in cerebellum granular neurons. Cell Mol Neurobiol. 2017;37(3):453–60.

19. Lee RS, Strahlendorf HK, Strahlendorf JC. Enhanced sensitivity of cerebellar Purkinje cells to iontophoretically-applied serotonin in thiamine deficiency. Brain Res. 1985;327(1–2):249–58.

20. Bowyer JF, Tranter KM, Sarkar S, Hanig JP. Microglial activation and vascular responses that are associated with early thalamic neurodegeneration resulting from thiamine deficiency. NeuroToxicology. 2018;65:98–110.

21. Inaba H, Kishimoto T, Oishi S, Nagata K, Hasegawa S, Watanabe T, et al. Vitamin B1-deficient mice show impairment of hippocampus-dependent memory formation and loss of hippocampal neurons and dendritic spines: potential microendophenotypes of Wernicke-Korsakoff syndrome. Biosci Biotechnol Biochem. 2016;80(12):2425–36.

22. Watanabe I. Pyrithiamine-induced acute thiamine-deficient encephalopathy in the mouse. Exp Mol Pathol. 1978;28(3):381–94.

23. Murdock DS, Gubler CJ. Effects of thiamine deficiency and treatment with the antagonists, oxythiamine and PYRI-thiamine, on the levels and distribution of thiamine derivatives in rat brain. J Nutr Sci Vitaminol. 1973;19(3):237–49.

24. Butterworth RF, Hamel E, Landreville F, Barbeau A. Amino acid changes in thiamine-deficient encephalopathy: some implications for the pathogenesis of Friedreich's ataxia. Can J Neurol Sci. 1979;6(2):217–22.

25. Jolicoeur FB, Rondeau DB, Hamel E, Butterworth RF, Barbeau A. Measurement of ataxia and related neurological signs in the laboratory rat. Can J Neurol Sci. 1979;6(2):209–15.

26. Shi Q, Karuppagounder S, Xu H, Pechman D, Chen H, Gibson G. Responses of the mitochondrial alpha-ketoglutarate dehydrogenase complex to thiamine deficiency may contribute to regional selective vulnerability. Neurochem Int. 2007;50(7–8):921–31.

27. Vetreno RP, Ramos RL, Anzalone S, Savage LM. Brain and behavioral pathology in an animal model of Wernicke's encephalopathy and Wernicke–Korsakoff syndrome. Brain Res. 2012;1436: 178–92.

28. Zhang S, Henderson S, Corso T. Excitotoxic cytopathology, progression, and reversibility of thiamine deficiency-induced diencephalic lesions. *J Neuropath Experiment Exp Neurol*. 1995;54(2): 255–67.

29. Edgerton JR, Reinhart PH. Distinct contributions of small and large conductance Ca2+-activated K+ channels to rat Purkinje neuron function. J Physiol. 2003;548(1):53–69.

30. Liu M, Alimov AP, Wang H, Frank JA, Katz W, Xu M, et al. Thiamine deficiency induces anorexia by inhibiting hypothalamic AMPK. Neuroscience. 2014;267:102–13.

31. Light KE, Hayar AM, Pierce DR. Electrophysiological and immunohistochemical evidence for an increase in GABAergic inputs and HCN channels in Purkinje cells that survive developmental ethanol exposure. Cerebellum. 2015;14(4):398–412.

32. Walter JT, Alviña K, Womack MD, Chevez C, Khodakhah K. Decreases in the precision of Purkinje cell pacemaking cause cerebellar dysfunction and ataxia. Nat Neurosci. 2006;9(3):389–97.

33. De Zeeuw CI, Chris I, Hoebeek FE, Bosman LWJ, Schonewille M, Witter L, Koekkoek SK. Spatiotemporal firing patterns in the cerebellum. Nat Rev Neurosci. 2011;12(6):327–44.

34. Shakkottai VG, do Carmo Costa M, Dell'Orco JM, Sankaranarayanan A, Wulff H, Paulson HL. Early changes in cerebellar physiology accompany motor dysfunction in the polyglutamine disease spinocerebellar ataxia type 3. J Neurosci. 2011;31(36):13002–14.

35. Llinás RR. Intrinsic electrical properties of mammalian neurons and CNS function: a historical perspective. Front Cell Neurosci. 2014;4(8):320. https://doi.org/10.3389/fncel.2014.00320.

36. Belmeguenai A, Hosy E, Bengtsson F, Pedroarena CM, Piochon C, Teuling E, et al. Intrinsic plasticity complements long-term potentiation in parallel fiber input gain control in cerebellar Purkinje cells. J Neurosci. 2010;30(41):13630–43.

37. Benton MD, Lewis AH, Bant JS, Raman IM. Iberiotoxin-sensitive and -insensitive BK currents in Purkinje neuron somata. J Neurophysiol. 2013;109(10):2528–41.

38. Cingolani LA, Gymnopoulos M, Boccaccio A, Stocker M, Pedarzani P. Developmental regulation of small-conductance Ca2+-activated K+ channel expression and function in rat Purkinje neurons. J Neurosci. 2002;22(11):4456–67.

39. Gähwiler BH, Llano I. Sodium and potassium conductances in somatic membranes of rat Purkinje cells from organotypic cerebellar cultures. J Physiol. 1989;417(1):105–22.

40. Gruol DL, Dionne VE, Yool AJ. Multiple voltage-sensitive K+ channels regulate dendritic excitability in cerebellar Purkinje neurons. Neurosci Lett. 1989;97(1–2):97–102.

41. Gruol DL, Jacquin T, Yool AJ. Single-channel K+ currents recorded from the somatic and dendritic regions of cerebellar Purkinje neurons in culture. J Neurosci. 1991;11(4):1002–15.

42. Sausbier M, Hu H, Arntz C, Feil S, Kamm S, Adelsberger H, et al. Cerebellar ataxia and Purkinje cell dysfunction caused by Ca2+-activated K+ channel deficiency. Proc Natl Acad Sci U S A. 2004;101(25):9474–8.

43. Womack MD, Khodakhah K. Somatic and dendritic small-conductance calcium-activated potassium channels regulate the output of cerebellar Purkinje neurons. J Neurosci. 2003;23(7): 2600–7.

44. Sacco T, Tempia F. A-type potassium currents active at subthreshold potentials in mouse cerebellar Purkinje cells. J Physiol. 2002;543(2):505–20.

45. Schreurs BG. Changes in cerebellar intrinsic neuronal excitability and synaptic plasticity result from eyeblink conditioning. Neurobiol Learn Mem. 2019;166(September):107094.

46. Grasselli G, He Q, Wan V, Adelman JP, Ohtsuki G, Hansel C. Activity-dependent plasticity of spike pauses in cerebellar Purkinje cells. Cell Rep. 2016;14(11):2546–53.

47. Grasselli G, Boele HJ, Titley HK, Bradford N, van Beers L, Jay L, et al. SK2 channels in cerebellar Purkinje cells contribute to excitability modulation in motor-learning–specific memory traces. PLoS Biol. 2020;18(1):1–29.

48. Adelman JP, Maylie J, Sah P. Small-conductance Ca 2+-activated K + channels: form and function. Annu Rev Physiol. 2012;74(1): 245–69.

49. Zhou H, Lin Z, Voges K, Chiheng J, Gao Z, Bosman LWJ, et al. Cerebellar modules operate at different frequencies. ELife. 2014;2014(3):1–18.

50. Wu B, Blot FGC, Wong AB, Osório C, Adolfs Y, Pasterkamp RJ, et al. TRPC3 is a major contributor to functional heterogeneity of cerebellar Purkinje cells. ELife. 2019;8:1–31.

51. Xiao J, Cerminara NL, Kotsurovskyy Y, Aoki H, Burroughs A, Wise AK, et al. Systematic regional variations in Purkinje cell spiking patterns. PLoS One. 2014;9(8):e105633. https://doi.org/10.1371/journal.pone.0105633.

52. Fox EA, Gruol DL. Corticotropin-releasing factor suppresses the afterhyperpolarization in cerebellar Purkinje neurons. Neurosci Lett. 1993;149(1):103–7.

53. Butterworth RF. Pathophysiology of cerebellar dysfunction in the Wernicke-Korsakoff syndrome. Can J Neurol Sci. 1993;20(SUPPL. 3):123–6.

54. Ohtsuki G, Piochon C, Adelman JP, Hansel C. SK2 channel modulation contributes to compartment-specific dendritic plasticity in cerebellar Purkinje cells. Neuron. 2012;75(1):108–20.

55. Titley HK, Watkins GV, Lin C, Weiss C, McCarthy M, Disterhoft JF, et al. Intrinsic excitability increase in cerebellar Purkinje cells after delay eye-blink conditioning in mice. J Neurosci. 2020;40(10): 2038–46.

56. Wang D, Schreurs BG. Characteristics of IA currents in adult rabbit cerebellar Purkinje cells. Brain Res. 2006;1096(1):85–96.

57. Hu C-L, Zeng X-M, Zhou M-H, Shi Y-T, Cao H, Mei Y-A. Kv 1.1 is associated with neuronal apoptosis and modulated by protein kinase C in the rat cerebellar granule cell. J Neurochem. 2008;106(3):1125–37.

58. Lefebvre T, Gonzalez BJ, Vaudry D, Desrues L, Falluel-Morel A, Aubert N, et al. Paradoxical effect of ethanol on potassium channel currents and cell survival in cerebellar granule neurons. J Neurochem. 2009;110(3):976–89.

59. Luo J. Mechanisms of ethanol-induced death of cerebellar granule cells. Cerebellum. 2012;11(1):145–54.

60. Cooper JR, Pincus JH. The role of thiamine in nervous tissue. Neurochem Res. 1979;4(2):223–39.

61. Brin M. Effects of thiamine deficiency and of oxythiamine on rat tissue transketolase. J Nutr. 1962;78(2):179–83.

62. Klooster A, Larkin JR, Wiersema-Buist J, Reinold OB, Gans PJ, Thornalley GN, et al. Are brain and heart tissue prone to the development of thiamine deficiency? Alcohol. 2013;47(3):215–21.

63. Savage LM, Hall JM, Resende LS (2012) Translational rodent models of Korsakoff syndrome reveal the critical neuroanatomical substrates of memory dysfunction and recovery. 195–209.

64. Dias FMV, de Freitas Silva DM, de Proença Doyle FC, Ribeiro AM. The connection between maternal thiamine shortcoming and offspring cognitive damage and poverty perpetuation in underprivileged communities across the world. Med Hypotheses. 2013;80(1):13–6.

65. Johnson CR, Fischer PR, Thacher TD, Topazian MD, Bourassa MW, Combs GF. Thiamin deficiency in low- and middle-income countries: disorders, prevalences, previous interventions and current recommendations. Nutr Health. 2019;25(2):127–51.

66. Iimura Y, Kurokawa T, Nojima M, Kanemoto Y, Yazawa K, Tsurita G, et al. Potential thiamine deficiency and neurological symptoms in patients receiving chemotherapy for gastrointestinal cancer. Int J Clin Pharmacol Therapeut. 2020;58(03):139–45.

67. Baker KG, Harding AJ, Halliday GM, Kril JJ, Harper CG. Neuronal loss in functional zones of the cerebellum of chronic alcoholics with and without Wernicke's encephalopathy. Neuroscience. 1999;91(2):429–38.

68. Kloss O, Michael Eskin NA, Suh M. Thiamin deficiency on fetal brain development with and without prenatal alcohol exposure. Biochem Cell Biol. 2018;96(2):169–77.

69. Nunes PT, Gómez-Mendoza DP, Rezende CP, Figueiredo HCP, Ribeiro AM. Thalamic proteome changes and behavioral impairments in thiamine-deficient rats. Neuroscience. 2018;385:181–97.

70. Jin XH, Wang HW, Zhang XY, Chu CP, Jin YZ, Cui SB, Qiu DL. Mechanisms of spontaneous climbing fiber discharge-evoked pauses and output modulation of cerebellar Purkinje cell in mice. Front Cell Neurosci. 2017;11:247. https://doi.org/10.3389/fncel.2017.00247.

71. Larsen JO, Tandrup T, Brændgaard H. The volume of Purkinje cells decreases in the cerebellum of acrylamide? Intoxicated rats, but no cells are lost. Acta Neuropathol. 1994;88(4):307–12.

72. Jaatinen P, Rintala J. Mechanisms of ethanol-induced degeneration in the developing, mature, and aging cerebellum. Cerebellum. 2008;7(3):332–47.

73. Gluber C. Studies on the physiological functions of thiamine. I. The effects of thiamine deficiency and thiamine antagonists on the oxidation of alphaketo acids by rat tissues . J Biol Chem. 1961;236: 3112–20.

74. Rindi G, Imarisio L, Patrini C. Effects of acute and chronic ethanol administration on regional thiamin pyrophosphokinase activity of the rat brain. Biochem Pharmacol. 1986;35(22):3903–8.